Desalination and Water Treatment
www.deswater.com

doi: 10.1080/19443994.2013.808396

52 (2014) 4453–4461
June

Taylor & Francis
Taylor & Francis Group

Lanthanides diffusion through pH-responsive reverse osmosis membranes

B. El-Gammal

Hot Laboratories Center, Atomic Energy Authority, P.O. 13759, Cairo, Egypt
Email: belalelgammal@hotmail.com

Received 12 February 2012; Accepted 1 May 2013

ABSTRACT

The adsorption of some lanthanides in the trivalent state, namely trivalent Ce, Pr, Sm, Gd, Dy, and Ho, was identified onto polyacrylamide zirconium titanosilicate (PAm-ZTS) composite membranes. Numerous opportunities for reverse osmosis-type separations involving organics that might become practical as suitable membrane systems became available. A theoretical framework for analysis of experimental data in terms of fundamental parameters was developed, to study the effect of the transport of the solute and solvent in the polymer membrane. Different theoretical modeling approaches were tested; Langmuir and Freundlich models appeared to have various regressions, so that Langmuir model was taken as the best fit theoretical model. During the polymer enhanced ultrafiltration, the tested retained lanthanides were ordered as $Ce^{4+} > Pr^{3+} > Sm^{3+} > Gd^{3+} > Dy^{3+} > Ho^{3+}$. Upon competing conditions, the Q_{max} values were decreased to nearly 50%.

Keywords: Adsorption; Reverse osmosis; Lanthanides; Diffusion; Solvent and pressure; Isotherms

1. Introduction

Polymer–inorganic nanocomposite membranes present a new concept to rectify the separation properties of polymer membranes because they hold properties of both organic and inorganic membranes such as good permeability, selectivity, mechanical strength, and thermal and chemical stability [1–6].

In the last two decades, significant ameliorations to the performance of polymeric membranes for ion separation have been made. Understanding the connections between the structure, permeability, and selectivity of these membranes has been greatly advanced [2,3]. Newer polymeric partition materials such as polyimides and cross-linked polyethylene glycol have been continuously developed [7–11]. Some polymeric membranes have already used in industry [12,13].

Polymeric membranes tend to be more cost-effective than other membranes because of their aptitude to be spun into hollow fibers or spiral-wound modules due to their flexibility and solution processability [1]. Despite these advantages and progresses, polymeric membranes are still constrained by the trade-off trend between ion permeability and selectivity, as suggested by Robeson [14].

Modifications of the chemical framework of a polymer often lead to an improvement in permeability at the cost of selectivity or vice versa [3]. Additionally, the segmental flexibility of polymeric membranes sometimes limits their ability to discriminate similar-sized penetrants, and they eventually lose performance stability at high temperatures [1]. On the other hand, inorganic membrane materials such as molecular

sieving materials usually rely on a difference in molecular size to achieve separation.

On a laboratory scale, these membranes show extremely appealing ion permeation and separation performance [15,16]. However, it is still troublesome and expensive to fabricate large membranes due to their fragile structures [1,2,17]. Therefore, polymeric membranes are even though inviting, but alternate approaches that can enhance their ion separation properties well above the Robeson line are needed. Polymer–inorganic nanocomposite materials, herein defined as inorganic nanofillers dispersed at a nanometer level in a polymer matrix, have been investigated for ion separation and have the potential to provide a way out to the trade-off problem of polymeric membranes [18,19]. For illustration, numerous polymer–inorganic nanocomposite membranes show much higher ion permeabilities but similar or even improved ion selectivity juxtaposed to the corresponding pure polymer membranes [20–26]. The nanocomposite materials may combine the advantages of each material: for instance, the flexibility and processability of polymers, and the selectivity and thermal stability of the inorganic fillers. Additionally, the ion separation performance of nanocomposite membranes can be further enhanced by chemical modification [27]. For instance, the introduction of organic functional groups on an inorganic filler surface sometimes contributes to not only a better dispersion of the inorganic material on the polymer membrane, but also a better absorption and transportation of penetrants, which results in favorable selectivity and permeability [27,28]. Membrane structure can be controlled by either the degree of cross-linking of the polymer matrix or the types of connection bonds between the polymer and inorganic phases in the nanocomposite material [28,29].

2. Experimental

2.1. Chemicals

Liquid Titanium(IV)chloride (98%)–$TiCl_4$, 189.68 [g/mol], 1.728 g/cm^3 (20˚C)—and Zirconium(IV)oxychloride octahydrate powder (>99.5%)–$ZrOCl_2.8H_2O$, 322.26752 [g/mol], 1.91 g/cm^3 (20˚C), pH value ~1 (50 g/l, H_2O, 20˚C)–were acquired from Merck Chemicals, Darmstadt, Germany. ACROS, USA tetraethylorthosilicate, $(C_2H_5O)_4Si$ 208.33 [g/mol], 0.93 g/cm^3 (20˚C) was used. All chemicals were used deprived of further purification, to be used throughout the preparation of the PAm-ZTS composite using liquid-phase synthetic routes. The polychelatogen used was polyethylenimine (PEI). This was received as a 50% by weight solution from Sigma-Aldrich (Cat No: 181978).

2.2. Synthesis of membranes

Because of the immense difference between the polymer and inorganic materials in their properties and strong aggregation of the nanofillers, polymer–inorganic nanocomposite PAm-ZTS membranes cannot be prepared by common schemes such as melt blending and roller mixing. The most commonly used preparation technologies for the fabrication of nanocomposite membranes can be divided into the following three types [30].

The sol–gel method is the most widely used preparation technology for nanocomposite membranes. Organic monomers, oligomers, or polymers and inorganic nanoparticle precursors are mixed together in the solution. The inorganic pioneers were mixed together by gradual addition of tetraethylortosilicate and dissolved in equal volumes of bidistilled water and ethyl alcohol with vigorous stirring to zirconium oxychlorideoctahydarte and titanium tetrachloride solutions, previously dissolved in concentrated hydrochloric acid. Then, they were hydrolyzed in a large amount of water after the condensation into well-dispersed nanoparticles in the polyacrylamide polymer matrix with different molar ratios. The advantage with this method is obvious: the reactions' conditions are moderate usually room temperature and ambient pressure, and the concentrations of organic and inorganic components are easy to control over the solution. Additionally, the organic and inorganic ingredients are dispersed at the molecular or nanometer level in the membranes, and thus, the membranes are homogeneous [32]. Other methods such as solution blending and *in situ* polymerization could be used [33–41].

3. Results and discussion

3.1. Morphology

Fig. 1(a) and (b) illustrates the photomicrograph of the cross-section and compact layer morphology of

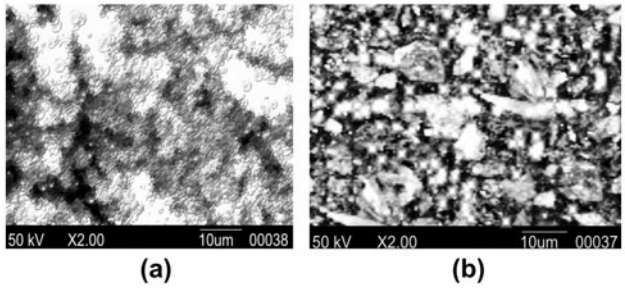

Fig. 1. (a) SEM of PAm-ZTS membranes at RT and (b) SEM of PAm-ZTS membranes at 250˚C.

dry/wet phase inversion shear-cast PAm-ZTS asymmetric membrane (forced convection dwelling time 15 s), at two different heating temperatures, 25 and 250 °C, separately. This structure had the relatively well-defined dense skin layer with invisible flaws supported on a highly porous open-celled sublayer containing not only micro-voids but also macro-voids. These were consistent with our expectation and appeared to be very similar to those found in the aqueous quenched asymmetric membranes observed by Pesek and Koros [18]. The macro-voids did not span the width of the membrane suggesting that these macro-voids are caused by different mechanisms. In this case, the creation macro-voids were believed to be formed by intrusion of non-solvent through defects in the skin layer during wet phase separation. This would lead to the reinforcement of the membranes. Also, no surface pores could be observed on the skin of flat sheet membrane, even at magnifications of 5,000×. This indicated that the diameters of any surface pores were less than 200 Å, which would be helpful for the ultrafiltration process.

3.2. Theory of ion exchange PAm-ZTS membranes

3.2.1. Retention of metal ions

The function of examination of the permeates samples for the relevant metal allows the calculation of the observed retention value (R_i) of each metal ion using:

$$R_i = \left(1 - \frac{C_{pi}}{C_{fi}}\right) \times 100 \quad (1)$$

where C_{pi} is the concentration of metal ion, i in the pass through and C_{fi} is the concentration of metal ion, i in the primary feed solution.

3.2.2. Langmuir and Freundlich isotherms

The utilization of Langmuir and Freundlich isotherms to depict the complexation process of binding metal ions in the polymer has previously been investigated using the washing and enrichment methods of the PEUF process [22,24]. In this case, the assumption that the concentration of metal ions in the permeates, C_{pi}, symbolizes the concentration of metal that is free in the solution, Y_i, is prepared.

The Langmuir isotherm equation is given by:

$$Q = \frac{Q_{max} \cdot Y_i}{K_L + Y_i} \quad (2)$$

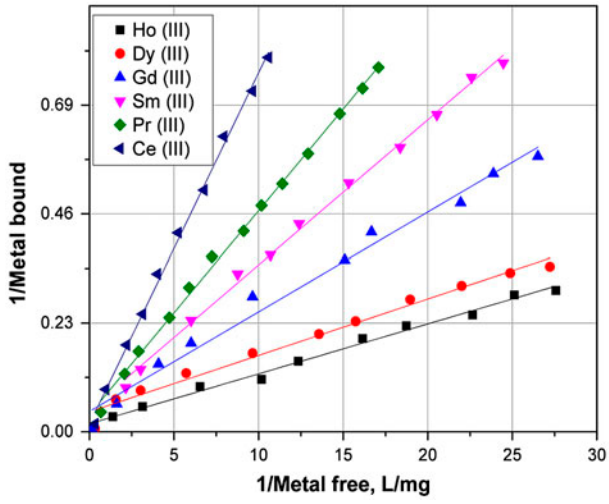

Fig. 2. Langmuir isotherm model fits to the experimental data for binding of single metal ions to PEI at pH 4.5 (polymer concentration = 1 g/l PEI).

where Q is the amount of metal bound (mg metal/g polymer); Q_{max} is the maximum capacity of polymer (mg metal/g polymer); Y_i is the metal free in solution (mg/l); K_L is the Langmuir equilibrium constant (mg/l).

Langmuir equation gives a linear form:

$$\frac{1}{Q} = \frac{K_L}{Q_{max}} \frac{1}{Y_i} + \frac{1}{Q_{max}} \quad (3)$$

The Freundlich isotherm equation is given by:

$$Q = K_F Y_i^n \quad (4)$$

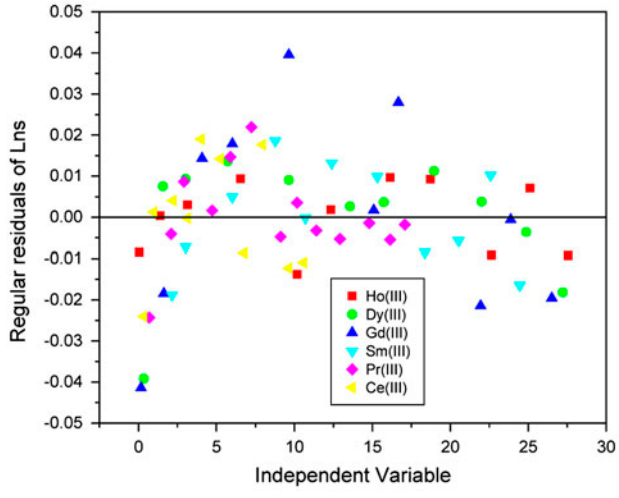

Fig. 3. Langmuir regular residuals for binding of single metal ions to PEI at pH 4.5 (polymer concentration = 1 g/l PEI).

Table 1
Values of the constants obtained by linear regression for single metal ions/polymer solutions for the Langmuir and Freundlich isotherms

Langmuir isothermal parameters				Freundlich parameters		
Exp.	Q_{max} (mg metal)/ (g_{PEI})	K_L (mg/l)	R^2	n	K_F ($mg^{1-n}\,g^{-1}\,l^n$)	R^2
Ce/PEI	165.5	20.3	0.999	0.94	6.0	0.995
Pr/PEI	67.6	10.2	0.999	0.78	4.1	0.994
Sm/PEI	53.2	1.56	0.999	0.55	12.3	0.937
Gd/PEI	20.2	1.44	0.997	0.35	7.0	0.766
Dy/PEI	17.6	0.76	0.989	0.35	6.0	0.882
Ho/PEI	12.3	2.18	0.995	0.45	2.87	0.968

where Q is the amount of metal bound (mg metal/g polymer); K_F is the Freundlich equilibrium constant ($mg^{1-n}\,g^{-1}\,l^n$); Y_i is the metal free in solution (mg/l); n is a constant.

Freundlich equation gives a linear form:

$$\ln Q = n \ln Y_i + \ln K_F \quad (5)$$

3.3. Study of single metals with PAm-ZTS binding and filtration

Figs. 2 and 3 display the linear regression fits of the Langmuir isotherm to the data obtained for particular metal ions in solution with PAm at pH 4.5. The Langmuir isotherm fitted the test data very well (R^2 values > 0.98, Table 1). Tables 2 and 3 show the detailed statistical Langmuir and Freundlich parameters for binding of single metal ions to PEI at pH 4.5 (polymer concentration = 1 g/l PEI). Figs. 4 and 5 exhibit the fits of the experimental data to the Freundlich isotherm. Although this model fits the data intelligently well, the fit was not as good as the Langmuir model as can be seen in Tables 1–3 and graphically represented in Figs. 3 and 5. This issue discloses that the Langmuir isotherm offers a better description of the binding of metal ions to the polymer than the Freundlich isotherm [31–36]. As can be seen in Table 1, the Q_{max} asset value was found in the following order:

$$Ce^{4+} > Pr^{3+} > Sm^{3+} > Gd^{3+} > Dy^{3+} > Ho^{3+}$$

These rates can be applicable when considering the retention of the metal ions during the ultrafiltration process.

3.4. Study of mixtures of metal ions with PAm-ZTS binding and filtration

Results from binding studies of single metal ion solutions, (Figs. 6 and 7), have shown the ability of

Table 2
Statistical parameters for binding of single metal ions to PEI at pH 4.5 (polymer concentration = 1 g/l PEI) using Langmuir model

$y = Ax + C$		Value	Standard error
Ho(III)	Intercept	0.01689	0.52143
Ho(III)	Slope	0.01057	0.03253
Dy(III)	Intercept	0.04219	0.52274
Dy(III)	Slope	0.01194	0.03293
Gd(III)	Intercept	0.04313	0.53856
Gd(III)	Slope	0.02104	0.0347
Sm(III)	Intercept	0.0464	0.61351
Sm(III)	Slope	0.03063	0.04071
Pr(III)	Intercept	0.03643	0.54514
Pr(III)	Slope	0.04302	0.05294
Ce(III)	Intercept	0.01587	0.57221
Ce(III)	Slope	0.07426	0.0936

Table 3
Statistical parameters for binding of single metal ions to PEI at pH 4.5 (polymer concentration = 1 g/l PEI) using Freundlich model

$y = Ax + C$		Value	Standard error
Dy(III)	Intercept	1.55489	0.3638
Dy(III)	Slope	0.54114	0.19695
Gd(III)	Intercept	2.93255	0.37212
Gd(III)	Slope	0.32755	0.15667
Sm(III)	Intercept	2.64327	0.43545
Sm(III)	Slope	0.94076	0.26161
Pr(III)	Intercept	3.88438	0.65313
Pr(III)	Slope	1.29011	0.48422
Ho(III)	Intercept	3.44668	0.35081
Ho(III)	Slope	0.32319	0.1517
Ce(III)	Intercept	4.45295	0.3475
Ce(III)	Slope	0.44738	0.15544

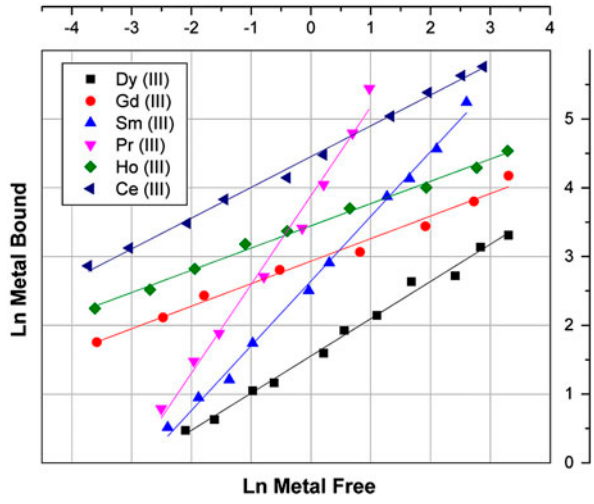

Fig. 4. Freundlich isotherm model fits to the experimental data for binding of single metal ions to PEI at pH 4.5 (polymer concentration = 1 g/l PEI).

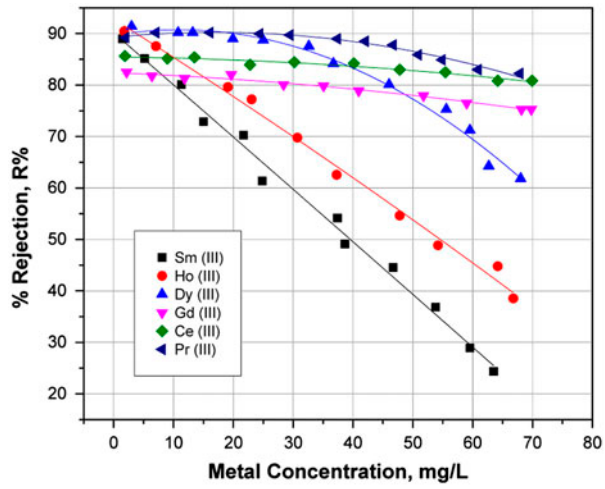

Fig. 6. Retention values of single metal ions at pH 4.5 in the presence of 1 g/l PEI for different feed metal concentrations using batch mode of PEUF.

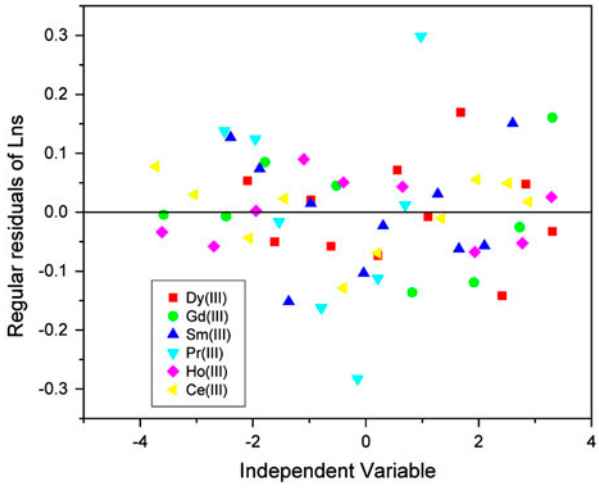

Fig. 5. Freundlich regular residuals for binding of single metal ions to PEI at pH 4.5 (polymer concentration = 1 g/l PEI).

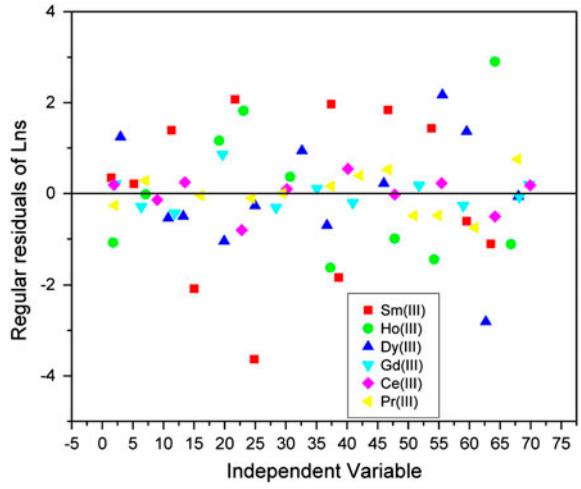

Fig. 7. Statistical regular residuals of single metal ions at pH 4.5 in the presence of 1 g/l PEI for different feed metal concentrations using batch mode of PEUF.

achieving maximum binding of metal ion to the polymer using batch mode PEUF with PEI as a polychelatogen. As an extension to the work carried out on simple aqueous solutions of particular metal ions, the competition effect of mixtures of metal ions in batch mode, PEUF was investigated. Langmuir and Freundlich isotherms were explored under competitive environment of mixtures of metal ion solutions with PAm [34].

Figs. 8–11 show the linear regression fits and their statistical residuals of the Langmuir and Freundlich isotherms to the data for mixtures of metal ions, respectively. The fitted data are described by linear equations that are represented in Tables 4–6; following trend for the Q_{max} values was found:

$$Ce^{4+} > Pr^{3+} > Sm^{3+} > Gd^{3+} > Dy^{3+} > Ho^{3+}$$

Matching the values in Tables 1 and 7, it can be seen that the Q_{max} values for Ce^{4+}, Sm^{3+}, Gd^{3+}, and Ho^{3+} fall off substantially (by 50% or greater) under competitive conditions, whereas the Q_{max} values for Pr^{3+} and Dy^{3+} remained very similar to the values for the unique metal ion polymer solutions. This suggests that $Pr^{3+}$and Dy^{3+} had unusual binding mechanisms

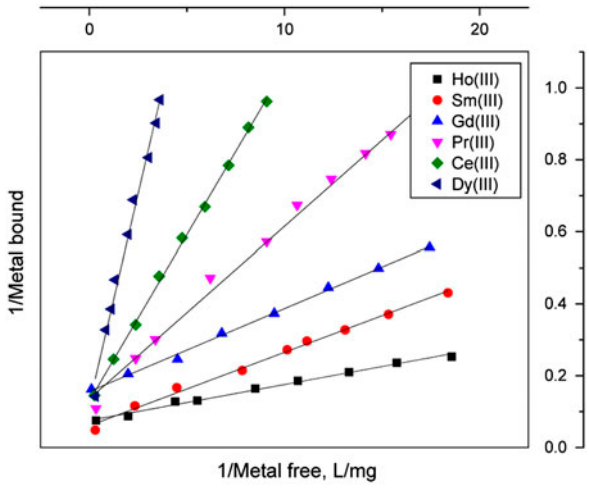

Fig. 8. Langmuir isotherm model fits to the experimental data for binding of mixtures of metal ions to PEI at pH 4.5 (polymer concentration = 1 g/l PEI).

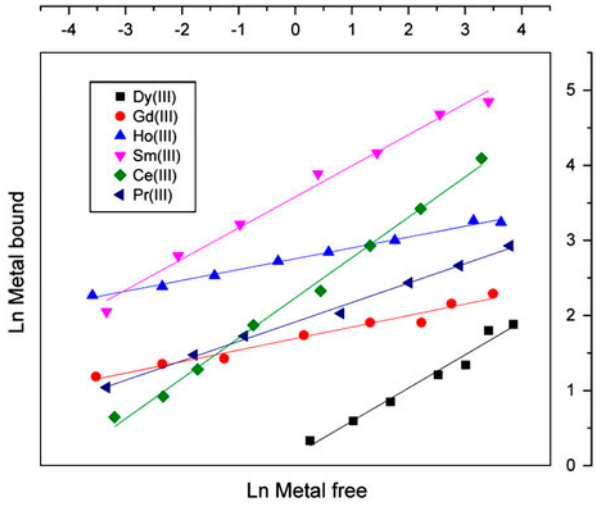

Fig. 10. Freundlich isotherm model fits to the experimental data for binding of mixtures of metal ions to PEI at pH 4.5 (polymer concentration = 1 g/l PEI).

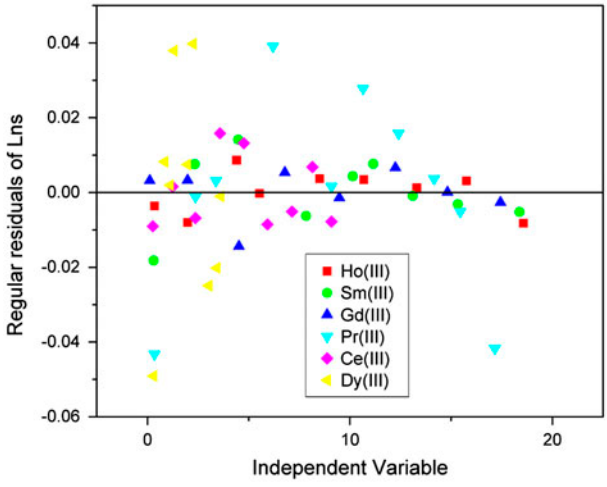

Fig. 9. Regular residuals of Langmuir isotherm model for binding of mixtures of metal ions to PEI at pH 4.5 (polymer concentration = 1 g/l PEI).

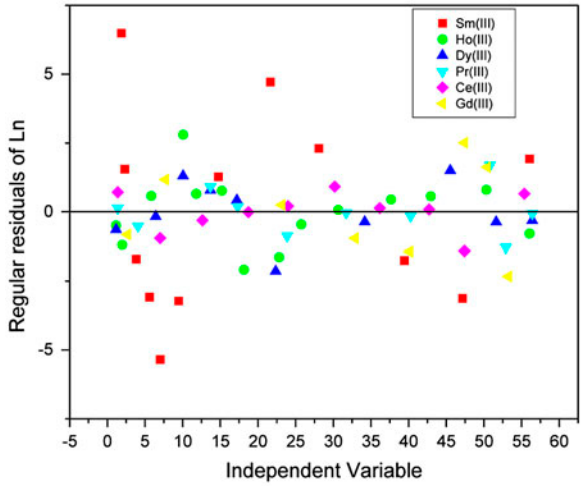

Fig. 11. Regular residuals of Freundlich isotherm model for binding of mixtures of metal ions to PEI at pH 4.5 (polymer concentration = 1 g/l PEI).

or bind to different sites than the other metal ions and so are not affected by the presence of these ions. However, Ce^{4+}, Sm^{3+}, Gd^{3+}, and Ho^{3+} all seem to be competing for the same binding sites within the polymer and are affected by the presence of other ions [39,40].

The holding rates as a function of metal concentrations under competitive conditions are shown in Figs. 12 and 13. Fitting the data revealed that the experimental parameters are set to give a second-order polynomial fit as given by Table 8. As can be seen, the correlation coefficients were changed according to the fitting procedures as recorded by their differences between Tables 7 and 8. The retention profiles for $Pr^{3+}$and Dy^{3+} were similar to those obtained for the individual metal ion/polymer solutions of these ions, showing no significant impact of metals competition on the retention of these ions. For the other metal ions, the highest retention was observed at low metal concentrations, with a dramatic drop in retention being contemplated as the concentration of the metal ions increases [37,38].

4. Conclusion

In a strive to recognize the end-result of metal ion competition on binding to PEI, PEUF experiments in the presence of single metal ions and mixtures of metal

Table 4
Fitting parameters due to retention of single metal ions at pH 4.5 in the presence of 1 g/l PEI for different feed metal concentrations using batch mode of PEUF

$y = B_1x^2 + B_2x + C$	Intercept		B1		B2		Statistics
	Value	Standard error	Value	Standard error	Value	Standard error	Adj. R^2
Sm(III)	90.1534	1.56306	−1.00924	1.18E−01	−1.50E−04	0.00175	0.99114
Ho(III)	92.80551	1.48422	−0.73262	9.97E−02	−9.48E−04	0.00137	0.99093
Dy(III)	89.65515	1.32041	0.197	8.82E−02	−0.0089	0.00118	0.98099
Gd(III)	82.40632	0.32253	−0.04651	0.02169	−8.33E−04	2.88E−04	0.97625
Ce(III)	85.47862	0.37849	−0.01387	0.02555	−7.89E−04	3.44E−04	0.93482
Pr(III)	89.27786	0.41298	0.11448	0.02689	−0.00337	3.78E−04	0.9694

Table 5
Statistical parameters of binding of mixtures of metal ions to PEI at pH 4.5 (polymer concentration = 1 g/l PEI) using Langmuir model

$y = Ax + C$	Intercept		Slope		Statistics
	Value	Standard error	Value	Standard error	Adj. R^2
Ho(III)	0.0756	0.00361	0.01001	3.41E−04	0.9908
Sm(III)	0.06099	0.00654	0.02042	6.03E−04	0.99306
Gd(III)	0.15614	0.00449	0.02308	4.40E−04	0.99746
Pr(III)	0.13582	0.01698	0.0479	0.00159	0.99016
Ce(III)	0.12952	0.00661	0.09246	0.00119	0.99868
Dy(III)	0.12007	0.02093	0.23398	0.00916	0.98787

Table 6
Statistical parameters of binding of mixtures of metal ions to PEI at pH 4.5 (polymer concentration = 1 g/l PEI) using Freundlich model

$y = Ax + C$	Intercept		Slope		Statistics
	Value	Standard error	Value	Standard error	Adj. R^2
Dy(III)	0.1527	0.07874	0.44061	0.03077	0.97144
Gd(III)	1.6919	0.0252	0.1533	0.0105	0.96804
Ho(III)	2.75526	0.0119	0.14429	0.00491	0.99196
Sm(III)	3.57852	0.04563	0.41298	0.01991	0.98622
Ce(III)	2.23421	0.03277	0.53593	0.01527	0.99434
Pr(III)	1.91344	0.01955	0.25875	0.00793	0.99439

Table 7
Values of the constants obtained by linear regression for mixtures of metal ions/polymer solutions for the Langmuir and Freundlich isotherms

Langmuir parameters				Freundlich parameters		
Exp.	Q_{max} (mg metal)/(g_{PEI})	K_L (mg/l)	R^2	n	K_F ($mg^{1-n}\,g^{-1}\,l^n$)	R^2
Ce/PEI	66.43	15.73	0.994	0.6	5.7	0.979
Pr/PEI	56.88	3.56	0.993	0.46	12.4	0.935
Sm/PEI	28.72	3.52	0.983	0.36	3.9	0.944
Gd/PEI	16.63	0.29	0.986	0.11	7.35	0.886
Dy/PEI	7.75	0.36	0.998	0.13	6.26	0.862
Ho/PEI	5.52	5.44	0.775	0.61	0.45	0.909

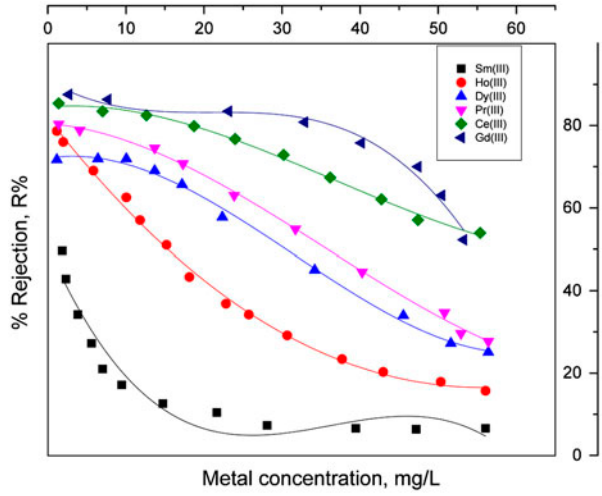

Fig. 12. Retention values of mixture metal ions at pH 4.5 in the presence of 1 g/l PEI for different feed metal concentrations using batch mode of PEUF.

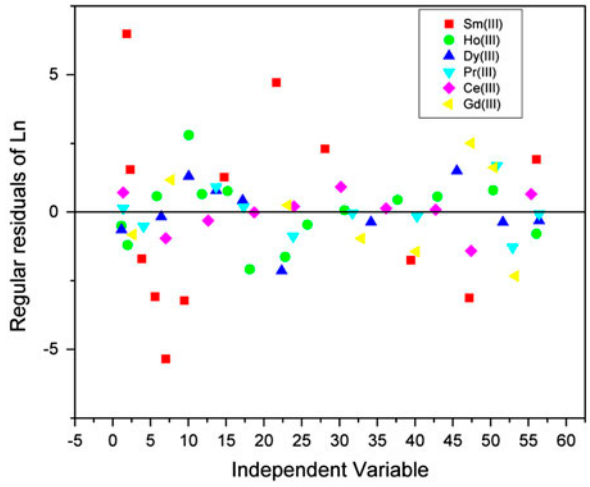

Fig. 13. Regular residuals of retention of metal ions mixture at pH 4.5 in the presence of 1 g/l PEI for different feed metal concentrations using batch mode of PEUF.

Table 8
Fitting parameters due to retention of metal ions mixture at pH 4.5 in the presence of 1 g/l PEI for different feed metal concentrations using batch mode of PEUF

$y = B_1x^2 + B_2x + C$	Intercept		B1		B2		B3		Statistics
	Value	Standard error	Value	Standard error	Value	Standard error	Value	Standard error	Adj. R^2
Sm(III)	50.67148	3.38394	−4.31969	0.66828	0.12952	0.02914	−0.0012	3.42E−04	0.92268
Ho(III)	81.97096	1.1216	−2.45672	0.18863	0.02496	0.00823	−3.51E−05	9.78E−05	0.99587
Dy(III)	72.0655	1.33875	0.30366	0.21011	−0.04969	0.00885	5.25E−04	1.03E−04	0.99548
Pr(III)	80.46618	1.00846	−0.13972	0.17292	−0.02988	0.00751	2.80E−04	8.76E−05	0.99746
Ce(III)	84.51311	0.96529	0.15867	0.15295	−0.02614	0.00636	2.36E−04	7.38E−05	0.99383
Gd(III)	91.00002	3.09935	−1.11611	0.59652	0.05336	0.02522	−8.50E−04	2.91E−04	0.96841

ions have been carried out. The results have been fitted to the Langmuir and Freundlich isotherms. The Langmuir isotherm provided a better fit to the data obtained than the Freundlich model for the R^2 values for the Langmuir fit being bigger than the values for the Freundlich fit. It was observed that the maximum amount of metal ions bound to the polymer, Q_{max}, for Ce^{4+}, Sm^{3+}, Gd^{3+}, and Ho^{3+} decreased substantially in solutions containing mixtures of metal ions when compared to the values obtained for single metal ion solutions. However, for Pr^{3+} and Dy^{3+}, no significant decrease was seen. These data suggest that the binding sites of Pr^{3+} and Dy^{3+} remained constant in competition while Ce^{4+}, Sm^{3+}, Gd^{3+}, and Ho^{3+} show changes in both binding capacity and equilibrium constant. The effectiveness of the PEUF process is heavily dependent on the concentration of competing metal ions, influencing both capacity and selectivity of these systems.

References

[1] Z. Salam, J. Ahmed, B.S. Merugu, The application of soft computing methods for MPPT of PV system: A technological and status review, Appl. Energy 107 (2013) 135–148.
[2] L. Li, L. Fan, M. Sun, H. Qiu, X. Li, H. Duan, C. Luo, Adsorbent for chromium removal based on graphene oxide functionalized with magnetic cyclodextrin–chitosan, Colloids Surf. B: Biointerfaces 107 (2013) 76–83.
[3] W. Kujawski, A. Sobolewska, K. Jarzynka, C. Güell, M. Ferrando, J. Warczok, Application of osmotic membrane distillation process in red grape juice concentration, J. Food Eng. 116 (4) (2013) 801–808.
[4] S. Phuntsho, S. Hong, M. Elimelech, H.K. Shon, Forward osmosis desalination of brackish groundwater: Meeting water quality requirements for fertigation by integrating nanofiltration, J. Membr. Sci. 436 (2013) 1–15.

[5] S. Gassara, W. Chinpa, D. Quemener, R.B. Amar, A. Deratani, Pore size tailoring of poly(ether imide) membrane from UF to NF range by chemical post-treatment using aminated oligomers, J. Membr. Sci. 436 (2013) 36–46.
[6] E. Kim, Y. Liu, M. Gamal El-Din, An in-situ integrated system of carbon nanotubes nanocomposite membrane for oil sands process-affected water treatment, J. Membr. Sci. 429(15) (2013) 418–427.
[7] R. Prasanth, N. Shubha, H. Hoon Hng, M. Srinivasan, Effect of nano-clay on ionic conductivity and electrochemical properties of poly(vinylidene fluoride) based nanocomposite porous polymer membranes and their application as polymer electrolyte in lithium ion batteries, Eur. Polymer J. 49(2) (2013) 307–318.
[8] D.A. Cameron, R. Bissessur, D.C. Dahn, Synthesis and characterization of poly(ethylene glycol amine) electrolytes and nanocomposites based on graphite, Eur. Polymer J. 48 (2012) 1525–1537.
[9] M.B. Patil, S.A. Al-Muhtaseb, E. Sivaniah, Nanocomposite membranes of silica and polysulfone for improved gas permeation, Procedia Eng. 44 (2012) 1011–1012.
[10] T.V. Duncan, Applications of nanotechnology in food packaging and food safety: Barrier materials, antimicrobials and sensors, J. Colloid Interface Sci. 363 (2011) 1–24.
[11] G.M. Ibrahim, B. El-Gammal, I.M. El-Naggar, Selectivity modification of sodium and cesium ions on silicon antimonite, Curr. Top. Colloid Interface Sci. 6 (2003) 159–164.
[12] S.A. Shady, B. El-Gammal, Diffusion pathways of sodium and cesium ions in the particles of titanium(IV) antimonite, Colloids Surf. A: Physicochem. Eng. Aspects 268 (2005) 7–11.
[13] B. El-Gammal, S.A. Shady, Chromatographic separation of sodium, cobalt and europium on the particles of zirconium molybdate and zirconium silicate ion exchangers, Colloids Surf. A: Physicochem. Eng. Aspects 287 (2006) 132–138.
[14] B. El-Gammal, G.M. Ibrahim, H.H. El-Nahas, Thermodynamic and sorption behavior of U(VI) and Th(IV) on unsaturated polyester–styrene polymeric beads, J. Appl. Polymer Sci. 100 (2006) 4098–4106.
[15] H.H. El-Nahas, F.H. Khalil, G.M. Ibrahim, B. El-Gammal, Preparation of unsaturated polyester-styrene beads using gamma irradiation and chemical polymerization routes for use in the recovery of some alkali metal ions, J. Appl. Polymer Sci. 104(2) (2007) 1149–1160.
[16] E.A. Hegazy, B. El-Gammal, F.H. Khalil, T.M. Mabrouk, Evaluation of anionic- and cationic-supported hydrogel membranes for sorption of Th(IV) and U(VI) ions from nitric acid medium, J. Appl. Polymer Sci. 102 (2006) 320–332.
[17] G.M. Ibrahim, F.H. Khalil, B. El-Gammal, Interaction of La^{3+} and Ce^{4+} with polyethylene and polypropylene polymeric matrices, J. Appl. Polymer Sci. 103 (2007) 2141–2151.
[18] G.M. Ibrahim, M.I. Ahmad, B. El-Gammal, Structural development of TMMA and SSQXN-8 as porous chelating resins, J. Appl. Polymer Sci. 113 (2009) 3038–3048.
[19] B. El-Gammal, G.M. Ibrahim, K.F. Allan, I.M. El-Naggar, Modeling the PAAc-AN-TV surface using ^{134}Cs and $^{152+154}Eu$ sorption, J. Appl. Polymer Sci. 113 (2009) 3405–3416.
[20] G.M. Ibrahim, B. El-Gammal, I.M. El-Naggar, Synthesis and characterization of novel materials tin potassium vanadate and zirconium potassium vanadate inorganic multi-component ion exchangers, Separ. Sci. Technol. 46 (2011) 664–678.
[21] G.M. Ibrahim, M.I. Ahmad, B. El-Gammal, I.M. El-Naggar, Selectivity sequence of multivalent lanthanides for their separation on antimonate based exchangers, Separ. Sci. Technol. 46 (2011) 2549–2565.
[22] B. El-Gammal, K.F. Allan, Ion exchange reversibility of some radionuclides on zirconium tungstosuccinate and zirconium tungstosalicylate at their solid-liquid interfaces, Sep. Sci. Technol. 47 (2012) 131–146.
[23] S.S. Metwally, B. El-Gammal, H.F. Aly, S.A. Abo-El-Enein, Removal and Separation of some radionuclides by polyacrylamide-based Ce(IV) phosphate from radioactive waste solutions, Sep. Sci. Technol. 46 (2011) 1808–1821.
[24] B. El-Gammal, S.S. Metwally, H.F. Aly, S.A. Abo-El-Enein, Verification of double-shell model for sorption of cesium, cobalt, and europium ions on polyacrylonitrile-based Ce(IV) phosphate from aqueous solutions, Desalin. Water Treat. 46 (2012) 124–138.
[25] L.C. Costa, Catalyst mediated method of interfacial polymerization on a microporous support, and polymers, fibers, films and membranes made by such method, US Patent 5,693,227 (1997).
[26] A. Kulkarni, D. Mukherjee, W.N. Gill, Flux enhancement by hydrophilization of thin film composite reverse osmosis membranes, J. Membr. Sci. 114 (1996) 39–50.
[27] W.E. Mickols, Method of treating polyamide membranes to increase flux, US Patent 5,755,964 (1998).
[28] S.D. Arthur, D. Wilmington, Reverse osmosis membranes of polyamideurethane, US Patent 5,085,777 (1992).
[29] Y. Zhou, S. Yu, M. Liu, C. Gao, Preparation and characterization of polyamideurethane thin-film composite membranes, Desalination 180 (2005) 189–196.
[30] A.L. Ahmad, B.S. Ooi, Properties-performance of thin-film composites membrane: study on trimesoyl chloride content and polymerization time, J. Membr. Sci. 255 (2005) 67–77.
[31] A.K. Ghosh, B.-H. Jeong, X. Huang, E.M.V. Hoek, Impacts of reaction and curing conditions on polyamide composite reverse osmosis membrane properties, J. Membr. Sci. 311 (2008) 34–45.
[32] P.W. Morgan, S.L. Kwolek, Interfacial polycondensation 2. Fundamentals of polymer formation at liquid interfaces, J. Polym. Sci. A, Polym. Chem. 34 (1996) 531–559.
[33] E.L. Wittbecker, P.W. Morgan, Interfacial polycondensation 1, J. Polym. Sci. A: Polym. Chem. 34 (1996) 521–529.
[34] D.R. Lide, CRC Handbook of Chemistry and Physics, 84th ed., CRC Press, New York, NY, 2003–2004.
[35] A.P. Rao, N.V. Desai, R. Rangarajan, Interfacially synthesized thin film composite RO membranes for seawater desalination, J. Membr. Sci. 124 (1997) 263–272.
[36] S.D. Jons, K.J. Stutts, M.S. Ferritto, W.E. Mickols, Treatment of composite polyamide membranes to improve performance, US Patent 5,876,602 (1999).
[37] Y.-N. Kwon, J.O. Leckie, Hypochlorite degradation of crosslinked polyamide membranes II. Changes in hydrogen bonding behavior and performance, J. Membr. Sci. 282 (2006) 456–464.
[38] N.M. Al-Bastaki, A. Abbas, Modeling an industrial reverse osmosis unit, Desalination 126 (1999) 33–39.
[39] N.M. Al-Bastaki, A. Abbas, Predicting the performance of RO membranes, Desalination 132 (2000) 181–187.
[40] J. Marriott, E. Sorensen, A general approach to modelling membrane modules, Chem. Eng. Sci. 58 (2003) 4975–4990.
[41] F.J. Sapienza, W.N. Gill, M. Soltanieh, Separation of ternary salt/acid aqueous solutions using hollow fiber reverse osmosis, J. Membr. Sci. 54 (1990) 175–189.
[42] M. Liu, S. Yu, J. Tao, C. Gao, Preparation, structure characteristics and separation properties of thin-film composite polyamide-urethane seawater reverse osmosis membrane, J. Membr. Sci. 325 (2008) 947–956.